



Evaluation of the solidification process in a double-tube latent heat storage unit equipped with circular fins with optimum fin spacing

Abdullah Bahlekeh¹ | Hosseinali Ramezani Mouziraji² | Hussein Togun³ |
Abolfazl Ebrahimmataj Tiji⁴ | Azher M. Abed⁵ | Hayder I. Mohammed⁶  |
Raed Khalid Ibrahim⁷ | Muataz S. Alhassan⁸ | Pouyan Talebizadehsardari⁹ 

¹Mechanical Engineering Department, Ege University, Izmir, Turkey

²Department of Mechanical Engineering, Tarbiat Modares University, Tehran, Iran

³Department of Biomedical Engineering, College of Engineering, University of Thi-Qar, Thi-Qar, Iraq

⁴Department of Mechanical Engineering, Semnan University, Semnan, Iran

⁵Air Conditioning and Refrigeration Techniques Engineering Department, Al-Mustaqbal University, Babylon, Iraq

⁶Department of Physics, College of Education, University of Garmian, Kalar, Iraq

⁷Department of Medical Instrumentation Engineering Techniques, Al-Farahidi University, Baghdad, Iraq

⁸Division of Advanced Nano Material Technologies, Scientific Research Center, Al-Ayen University, Thi-Qar, Iraq

⁹Centre for Sustainable Energy Use in Food Chains, Institute of Energy Futures, Brunel University London, Uxbridge, UK

Correspondence

Abdullah Bahlekeh, Mechanical Engineering Department, Ege University, Bornova, Izmir, Turkey.
Email: a.bahlekeh@hotmail.com

Pouyan Talebizadehsardari, Centre for Sustainable Energy Use in Food Chains, Institute of Energy Futures, Brunel University London, Kingston Ln, Uxbridge UB8 3PH, UK.

Email: pouyan.talebizadehsardari@brunel.ac.uk; ptsardari@gmail.com

Abstract

In this study, the effect of fin number and size on the solidification output of a double-tube container filled with phase change material (PCM) was analyzed numerically. By altering the fins' dimensions, the PCM's heat transfer performance is examined and compared to finless scenarios. To attain optimal performance, multiple inline configurations are explored. In addition, the initial conditions of the heat transfer fluid (HTF), including temperature and Reynolds number, are considered in the analysis. The research results show a significant impact of longer fins with higher numbers on improving the solidification rate of PCM. The solidification rate increases by 67%, 170%, 308%, and 370% for cases with 4, 9, 15, and 19 fins, respectively, all with the same fin length and initial HTF boundary condition. The best case results in a solidification time that is 4.45 times shorter compared to other fin number and dimension scenarios. The study also found that moving from Reynolds numbers 500 to 1000 and 2000 reduced discharging times by 12.9% and 22%, respectively, and increased heat recovery rates by 14.4% and 27.9%. When the HTF entrance temperature was 10°C and 15°C, the coolant temperature showed that the entire discharging time decreased by 37.5% and 23.1% relative

This is an open access article under the terms of the Creative Commons Attribution License, which permits use, distribution and reproduction in any medium, provided the original work is properly cited.

© 2023 The Authors. *Energy Science & Engineering* published by the Society of Chemical Industry and John Wiley & Sons Ltd.

to the solidification time when the initial temperature was 20°C. Generally, this work highlights that increasing the length and number of fins enhances thermal efficiency and the phase change process.

KEYWORDS

circular fins, double-pipe heat exchanger, optimum fin spacing, phase change materials, solidification, thermal energy storage

1 | INTRODUCTION

Since the world is running out of fossil fuel resources, governments, municipalities, and policymakers tend to bring forward novel renewable-based energy systems to tackle the problem of greenhouse gas emissions from burning fossil fuels and supplying the required energy for buildings.¹⁻³ In this regard, renewable-based energy systems need to be developed.^{4,5} However, such systems mainly suffer from intrinsic flaws, including intermittency and low thermal efficiency.^{6,7} To address this problem, energy storage mechanisms such as batteries,^{8,9} chemical storage,^{10,11} pumped hydropower,¹² thermal energy storage (TES),^{13,14} and so forth, are being developed. More to the point, using energy storage mechanisms makes the energy systems reliable by quickly responding to impulsive fluctuations in power and supply needs and alleviating the secondary backup power plants.¹⁵ Since each energy storage mechanism has merits, the use of TES has been more widespread among all for engineering problems. This is due to their intrinsic features such as fair cost-effectiveness, cleanliness, capability to rapidly offset the energy gap and flexibility in integrating any energy systems.¹⁶ TES units typically consist of phase change transition substances encompassed in a tank and are supposed to store the extra thermal energy of the system when the source of renewable energy exists and then transfer the stored heat to the system when the source of energy vanishes.¹⁷ In this mechanism, the heat can be stored in these three forms sensible heat, latent heat, and thermochemical process. Latent heat storage (LHS) is highly preferred due to its higher energy density.¹⁸ One of the most valuable applications of TES units is in double/triple pipe heat exchangers where they are employed to save the heat during daytime and release it during the nighttime or cloudy weather when the solar energy disappears. This latent heat is stored in a phase change substance which is well-known as phase change material (PCM).^{19,20} LHS superiority in energy density and temperature stability over sensible heat storage makes it a better fit for applications requiring ample energy storage and consistent temperatures over long periods. One such use is in

TES systems of solar thermal power plants, where LHS enables efficient storage of large amounts of solar energy during the day for use in generating electricity at night or during low solar radiation.²¹

Although PCMs have engaged the researcher's interest, they regularly suffer from low thermal conductivity and low thermal diffusion rates, prohibiting their widespread usage.²² To solve this problem, scholars have been examining different techniques such as nanoparticle distribution within the heat transfer fluid (HTF),^{23,24} channel modification,^{25,26} the use of extended surfaces,^{27,28} and composite PCMs^{29,30} to improve thermo-physical properties of the PCM.³¹ For this issue, Khajuria et al.³² examined the effect of channel geometry on the heat transfer enhancement of a specific type of bio-PCM (honeybee wax) as a heat storage medium encompassed in the double pipe heat exchanger. They provided the 20 × 40 mm vertical eccentricity with upward and downward directions to the inner side of the heat exchanger tube to see the heat transfer behavior. According to their results, downward eccentricity enhances the charging rate of the bio-PCM; however, it prolongs the discharge process. On the other hand, upward eccentricity declines the charge/discharge rates as opposed to the concentric inner tube case. Fallah Najafabadi et al.³³ considered a concentric double pipe heat exchanger with helical coils, which circulates the turbulent HTF flows, and RT-50 as a PCM preserved in an annulus shape tanker. They also simulated the heat exchanger in a three-dimensional (3D) model and employed K-epsilon turbulent model to compute the Reynolds stress value. Their study aimed to consider the effect of critical geometrical parameters like helical pitch and inner/outer pipe diameter. According to their achievements, the helical pitch does not significantly influence the melting/solidification process, while the inner pipe diameter positively affects the melting behavior. Another helpful technique that can make up for the low thermal conductivity of PCMs is the use of nanoparticles. In this regard, Ho et al.³⁴ employed aluminum oxide as a nanoparticle dispersed within the PCM tanker placed in a concentric double pipe duct to enhance the heat storage rate of the PCM. They reported that aluminum oxide was capable of increasing the heat

storage capacity. Similar results were reported regarding nanoparticle dispersion within the base fluid.^{35,36}

Another viable approach by which the natural convection effect is improved in a latent heat energy storage system is the implementation of fins within the PCM container. In this context, Pássaro et al.³⁷ investigated a double-pipe heat exchanger equipped with PCM and fins. Their study was performed in a 3D state, and the heat flow was also considered transient and turbulent. Paraffin wax, in which graphene nanoplatelets were inserted, was also considered a phase-changing transition substance stored in a tank. In their study, parameters such as paraffin wax thermal properties, fin pitch and nanoparticle distribution within the HTF were employed to improve the discharge heat transfer rate. They concluded that the discharge rate of a finned tube heat exchanger with a well-suited fin pitch is superior to the case with nanoparticle distribution. In a similar study, Abidi et al.³⁸ employed calcium chloride hexahydrate ($\text{CaCl}_2 \cdot 6\text{H}_2\text{O}$) as a nano-PCM, in which graphene nanoparticles were spread in a finned double tube heat exchanger to improve the nano-PCM charge and discharge rate. They also found that fin length significantly impacts the melting and solidification process. According to their findings, an increase in fin length causes more uniform heat distribution leading to uniform charge and discharge rate. Sanchouli et al.³⁹ carried out to improve the thermal efficiency of a double pipe heat exchanger equipped with a specific type of PCM. For this purpose, they employed novel grid annular fins containing straight and circular strip elements on the inner tube side of the heat exchanger and compared their results with primary annular fins. They found that the geometrical features of the fins, like fin spacing and pitch, directly impact the amount of thermal energy stored by the PCM. According to their results, the substitution of novel grid annular fins could increase the heat storage capacity of the PCM by 69% at most, compared with conventional annular fins. In line with the strategy mentioned above, fin configuration is essential for a superior heat transfer rate to the PCM. In this regard, Singh et al.⁴⁰ experimentally investigated the effect of V-shaped twisted tape inserted on a double-pipe heat exchanger equipped with PCM and nanoparticle distribution. Their study aimed to determine the effect of geometrical parameters of twisted tape, such as twist ratio, depth ratio, and width ratio, on the heat transfer augmentation, entropy generation, and melting/solidification rate of the PCM. They found that the simultaneous decrease in twisting ratio and increase in particle concentration would considerably enhance the heat transfer rate to the PCM and heat storage capacity. They also reported that nanoparticles are likely to

increase the entropy generation compared to the case when no nanoparticle is involved. Yan et al.⁴¹ investigated the effect of V-shaped fin structure parameters such as angle, length, number, and their alignments on the heat storage capacity of the PCM. In their study, 17 V-shaped configurations were taken into account, and the response surface method was used to reach the optimum state of the art configuration. According to the results, the V-shaped structure has improved the melting rate of the upper part corner due to better natural convection. Also, it was reported that the melting time of the lower part of the PCM container where no fin is added took 62.5% of the total melting time, while the upper part contacting V-shaped fins only allocated 37.5% of the total melting time. Similarly, Deng et al.⁴² put efforts into optimizing the fin layout in a double-pipe heat exchanger equipped with PCM. They also compared no fins, straight fins, angled fins, lower fins, and upper fins cases to introduce the optimum design based on the Reynolds and Nusselt numbers. According to their findings, the best layout for when the Nusselt number is less than 6 is the lower fin case, while, for values greater than 6, an angled fin structure is the best approach. Baba et al.⁴³ experimentally investigated the amount of forced convection heat transfer enhancement due to adding internal longitudinal fins within the tube channel. They found the use of a finned tube heat exchanger. However, it increases the heat storage capacity. This enhances the natural convection effects and poses a higher pressure drop and friction factor due to creating higher resistance to the flow, compared with a plain tube heat exchanger. Also, there are other studies addressing the effects of fin configuration on the heat transfer rate and melting/solidification process of a double pipe heat exchanger that released similar reports.^{44,45}

As mentioned in the literature review, there are several studies on the effect of fin arrangement in double pipe heat storage systems. However, since the literature covers and to the best of the author's knowledge, most studies have outlined the effect of high conductivity surfaces on the PCM melting process. At the same time, less effort was performed with a focus on the solidification process. The effect of geometrical parameters of the extended surfaces on natural convection is not only limited to pitch length but also they have a reciprocal relationship with velocity, Reynolds, and Nusselt numbers, which has not yet been fully addressed. Thus, this paper investigates the effect of full geometrical parameters of circular fins and the state of the art layout of the best case, along with sensitivity analysis. For this purpose, a comprehensive evaluation on the performance of a vertical finned double-pipe LHS system is performed

during the solidification process. The unique feature of this study is that the total volume of the fins is considered constant in addition to the volume of the PCM so that various configurations can be compared meaningfully based on heat transfer enhancement capability and storage capacity. For this purpose, the length to width ratio of the fins is changed based on the length and number of the fins. It should be noted that the array of the fins is targeted in a double pipe heat exchanger as one of the most applicable heat exchangers in industries.

2 | PROBLEM DESCRIPTION

The optimum productivity during the discharge process is determined in this inquiry by analyzing a vertical double tube latent heat system (DTLHS) thermal exchanger with rectangular fins, as illustrated in Figure 1A. Once the coolant (water) is passed through the unit from the inner tube, the PCM starts the solidification process in the outer tube. The extended surfaces (fins) are connected to the internal tube within a PCM region to deliver energy from the PCM to the coolant. The DTLHS unit has an inner and outer radius of 10 and 20 mm, respectively, and a height of 250 mm. In fact, for the fixed space for the thermal exchanger and PCM, the physical properties of the fins are evaluated for the improvement procedure while taking a fixed volume for the fins. The fins' dimensions and numbers are measured concerning their physical features. Since the volume of the fins is fixed and based on the physical dimensions, the surface area is related to the length of the fin more than the width, so the assessments in this research were carried out using the fin's length. A sensitivity evaluation is likewise achieved for the

operating fluid's properties, such as temperature and flow rate, presented by Reynolds number, in parallel with the physical dimensions. It is emphasized that the numerical model is thought to be axisymmetric because of the structure under study and the absence of circular flow, as shown in Figure 1B, which also shows the volume of the domain.

2.1 | Boundary and initial conditions

Operating fluid has a consistent initial velocity and temperature. The outlet for the HTF may additionally have a pressure outlet. An adiabatic boundary condition is selected for the PCM enclosure to counteract environmental effects. Copper describes the middle wall separating the PCM from the working fluid. The central wall is 2-mm thick since the inner and outer tubes are 1-mm thick. For the walls, the no-slip boundary requirement is also taken into account. The PCM and HTF's initial temperatures are 50°C and 20°C. The temperature of the HTF is selected based on the phase change temperature of the PCM and is kept 1°C lower than the critical temperature of the PCM.

2.2 | Geometrical parameters and materials' properties

Considering nine fins, three distinct lengths for the fins (5, 10, and 15 mm) are selected. The volume of the fins remained constant throughout the study, as demonstrated by the adjustment of the thickness of the fins when the length increased from 5 to 10 and 15 mm. This ensures that the volume of the PCM remains consistent,

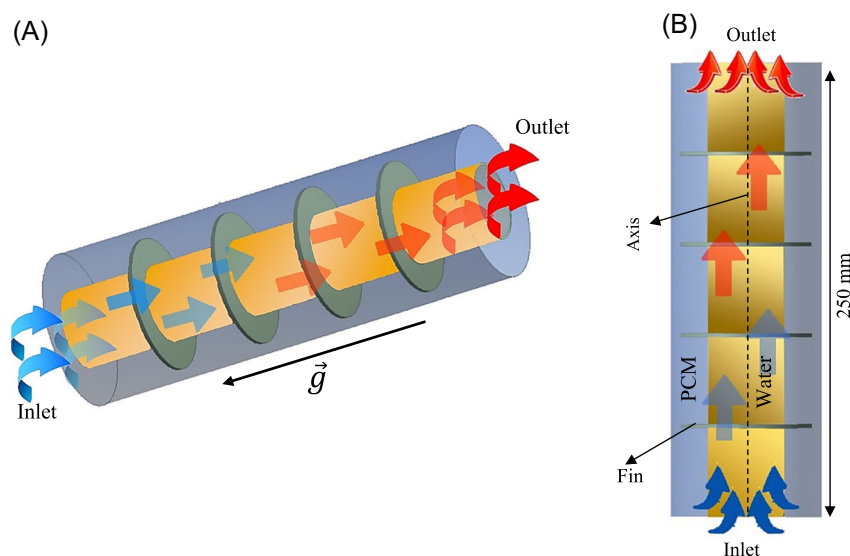


FIGURE 1 The schematic of the system in (A) three-dimensional (3D) and (B) 2D axisymmetric model.

TABLE 1 Thermodynamic characteristics of the applied PCM (RT35).³⁰

Properties	Values
ρ_l	770 kg/m ³
ρ_s	860 kg/m ³
C_p	170 kJ/kg K
L_f	2 kJ/kg
K	0.2 W/m K
μ	0.023 N s/m ²
T_L	36°C
T_S	29°C
β	0.0006 K ⁻¹

Abbreviation: PCM, phase change material.

providing a controlled environment for the examination of the effects of fin length on the performance of the TES system. After analyzing the impact of the fin's length, various values of 4, 9, 15, and 19 mm are explored. Re and coolant input temperature are taken into account when analyzing the parameters of the fin; they are 1000 and 15, respectively. The working fluid, considered water, is finally selected for the optimistic outcome using various Re of 500, 1000, and 2000 and varied input temperatures of 10°C, 15°C, and 20°C. It should be mentioned that depending on the water's entry temperature, the properties of the water alter.

RT35 was chosen as the PCM in this study, and Table 1 shows the characteristics. RT35 is a suitable PCM for solar energy applications as well as for building HVAC systems. In solar systems, the temperature of the working fluid in a collector can reach 35–40°C or even higher, which can be then stored in the storage system with RT35 PCM. In building applications such as underfloor heating systems, the working fluid temperature is in the range of 30–40°C. Furthermore, the thermal storage unit with RT35 PCM can be used to preheat the water temperature in other building heating systems such as radiators.

3 | MATHEMATICAL MODELING

The enthalpy approach developed by Brent et al.^{46,47} was used to depict the PCM phase change process. In this method, it was presumed that the liquid portion would cover every cell in the computational field upon startup. To formulate a numerical solution, the following statements are suggested^{48,49}:

1. Considering the density difference by applying the Boussinesq approximation.
2. 2D axisymmetric method for the computational field.
3. Transient, laminar, and incompressible fluid flow for the liquid PCM and HTF.
4. Applying gravity in the downward direction.
5. No velocity slips at solid boundaries.

Thus, the continuity, momentum, and energy are given as⁵⁰:

$$\frac{\partial \rho}{\partial t} + \nabla \cdot \rho \vec{V} = 0, \quad (1)$$

$$\rho \frac{\partial \vec{V}}{\partial t} + \rho (\vec{V} \cdot \nabla) \vec{V} = -\nabla P + \mu (\nabla^2 \vec{V}) - \rho \beta (T - T_{ref}) \vec{g} - \vec{S}, \quad (2)$$

$$\frac{\rho C_p \partial T}{\partial t} + \nabla (\rho C_p \vec{V} T) = \nabla (k \nabla T) - S_L. \quad (3)$$

The parameter (\vec{S}) in Equation (2) is included in calculating the effect of phase change on momentum, as⁵¹:

$$\vec{S} = A_m \frac{(1 - \lambda)^2}{\lambda^3 + 0.001} \vec{V}. \quad (4)$$

The factor of the mushy area A_m is set as 10^5 , depending on the literature.^{52,53} To assess the phase transition progression, λ (fluid part of PCM) is revealed as⁵⁴:

$$\lambda = \frac{\Delta H}{L_f} = \begin{cases} 0 & \text{if } T < T_S \\ 1 & \text{if } T > T_L \\ \frac{T - T_S}{T_L - T_S} & \text{if } T_S < T < T_L \end{cases}. \quad (5)$$

The source term S_L in the energy method is defined as:

$$S_L = \frac{\rho \partial \lambda L_f}{\partial t} + \rho \nabla (\vec{V} \lambda L_f). \quad (6)$$

The heat stored rate is measured as:

$$\dot{E}_T = \frac{E_{\text{end}} - E_{\text{ini}}}{t_m}, \quad (7)$$

where t_m is the charging time and E_e and E_i are the whole PCM's energy at the melting process's start and

endpoints. E is the total heat and $MC_p dT$ is sensible and ML_f is the latent cases of the PCM.

4 | NUMERICAL MODEL

To analyze the heat transfer efficiency of the PCM system, numerical simulations were run using the FLUENT software and a simple algorithm. The author's early work revealed further specifics of the numerical procedure. Software called ANSYS Designmodeler was used to create the mesh. This research ought to be carried out in advance of the primary research to ensure the problem's independence from the mesh size and time step size. Several mesh sizes of 0.1, 0.2, and 0.4 mm are initially considered. The findings of the comparison between the solidification time and heat recovery rate are shown in Table 2. The findings are virtually identical, as demonstrated, and the variation is negligible. The mesh size of 0.2 mm is therefore chosen for further study because there is hardly any variation between the sizes of 0.1 and 0.2 mm. Table 2 investigates the difference in a time step. As can be seen, the outcomes for time-step values of 0.05 and 0.1 s are nearly identical; hence, 0.1 s was selected as the time-step value.

The current findings are validated with the experimental assessment of Al-Abidi et al.⁵⁵ during solidification. They looked at the PCM temperature profile in a triple-pipe PCM-based cooling system with fins running its length. Four fins were added to the inner and outer tubes in the PCM domain (eight fins in total) in the staggered configuration to improve the heat transfer. The inner and outer diameters of the pipe were 25.4 and 75 mm, respectively. The total mass of the PCM was 5.6 kg. To determine the temperature in various places, 15 thermocouples were used to capture the temperature of the entire domain. The research work and those presented by Al-Abidi et al.⁵⁵ have an excellent correlation, as shown in Figure 2, which displays the average thermal gradient. Compared to the empirical observations, the current model successfully forecasts the discharging phenomenon.

TABLE 2 Mesh and time step size analysis.

Mesh size (mm)	0.1	0.2	0.4		
Time step size	0.1	0.05 s	0.1 s	0.2 s	0.1
Solidification time (s)	5865	5872	5884	5674	5726
Heat recovery rate (W)	28.88	28.91	29.03	30	29.81

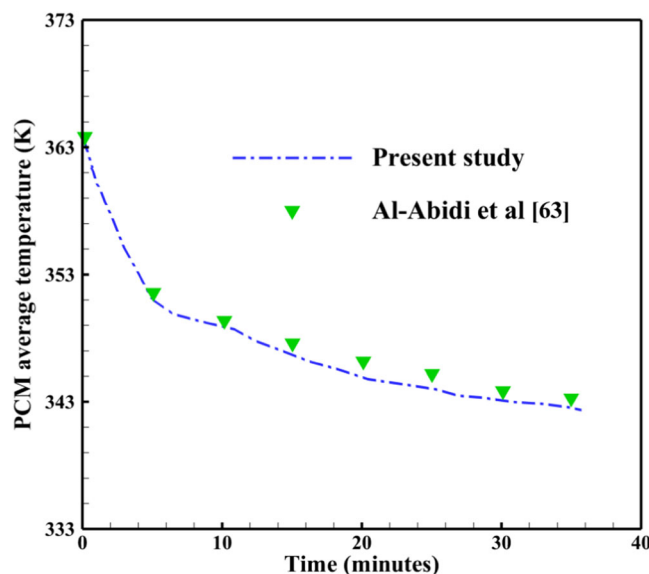


FIGURE 2 Code verification during the solidification process using the experimental study of Al-Abidi et al.⁵⁵

5 | RESULTS AND DISCUSSIONS

In the present study, many effective characteristics were considered to evaluate the impact of utilizing fins to improve PCM solidification. The impact of the fins' presence was explored by comparing the performance of the TES system with fins to a system with no fins.

5.1 | Effect of fin height

Figure 3A compares the solidification processes of the systems without and with fins at various dimensions (the number and the size of the fins are constant for all the cases). In the first row of Figure 3A, the solidification of the HTF without fins is displayed during a range of time increments from 300 to 5400 s. The PCM solid component was initially generated beside the HTF wall. As the domain solidified, it was discovered that the bottom-made PCM solid section was larger than the top-created PCM solid portion due to the buoyancy and gravity force. It is apparent that the solid phase layer of PCM has gotten thicker and thicker over time. The efficiency of the solidification process is improved by adding fins to the TES unit by expanding the heat transfer surface area and the effective thermal conductivity since the metal fins' thermal conductivity is greater than the PCMs. The PCM solid section grows initially, taking on the form of a fin. Due to the presence of fins, PCM that is in close enough proximity to or in direct touch with fins solidifies more quickly. The actual heat conduction between the fins and the PCM transitions into the direct heat conduction of

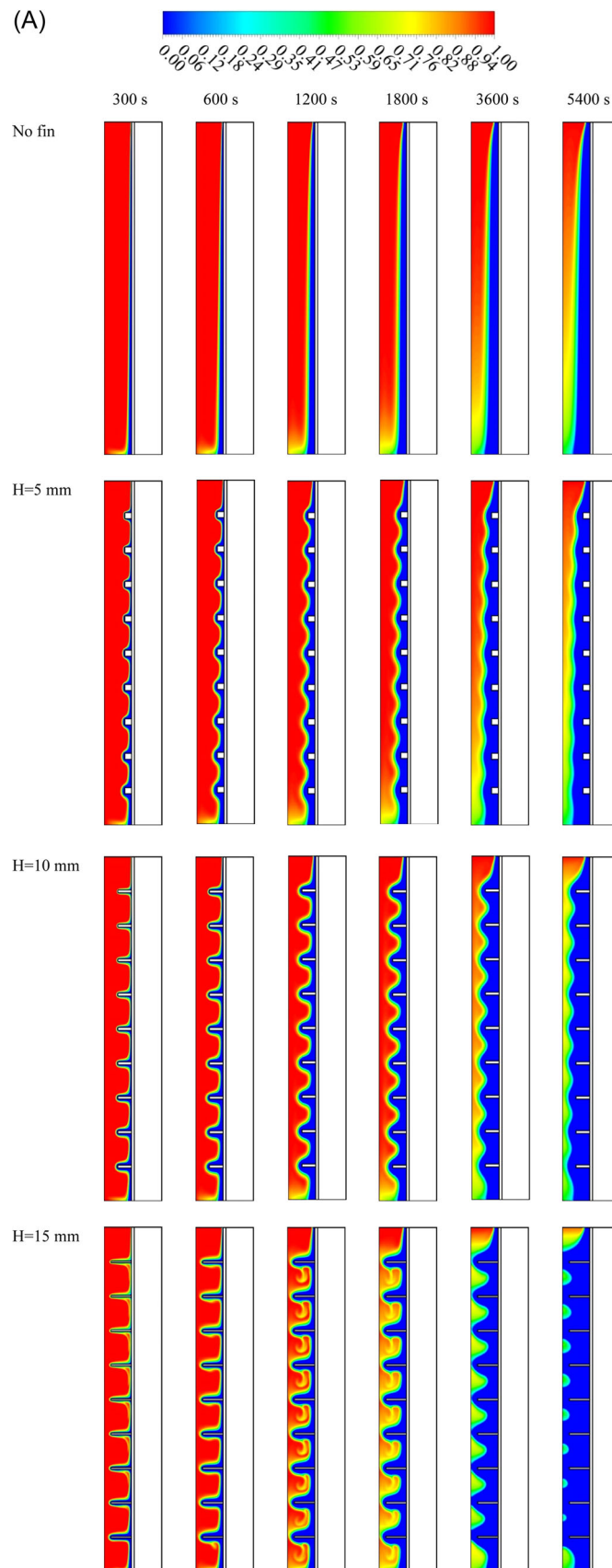


FIGURE 3 (A) Liquid fraction and (B) temperature distributions of the phase change material for various fin lengths at different time steps.

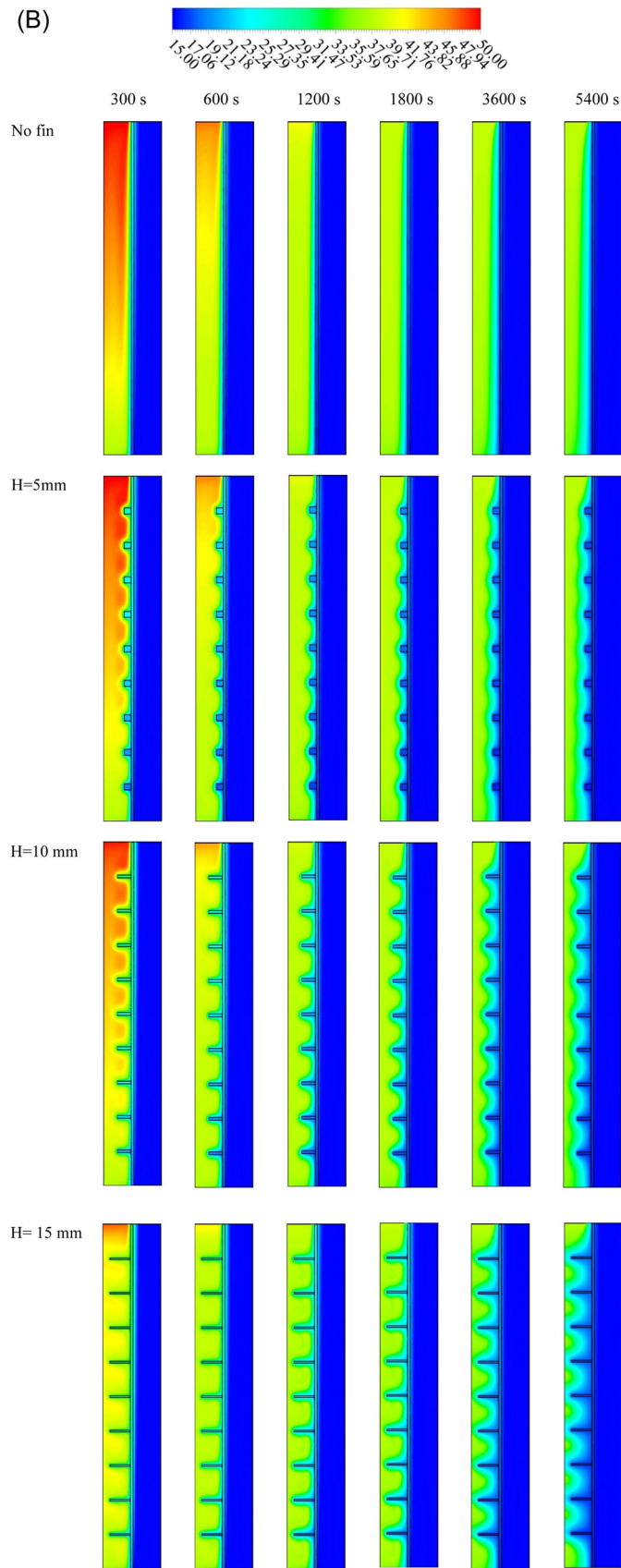


FIGURE 3 Continued

the solidified PCM to the non-solidified section as the solid phase layer of the PCM, however, becomes thicker and thicker over time. During this step, the solidification process slows down because most of the heat transfer during solidification is produced by the temperature differential between the liquid PCM and the solid PCM. Generally, the results found that the increase in PCM solid section gradually from the bottom side towards the top side with an increase in the period for all the cases. Different heights of fins ($H = 5$ mm, $H = 10$ mm, and $H = 15$ mm) were utilized to evaluate the impact of solidification processes. As fin height increases, heat transfer surface area increases, transferring more heat from the PCM section zone. Compared to other cases, the PCM solid rate variation rate was larger at $H = 15$ mm, indicating that the solidification rate occurred more quickly due to the enlarged heat transfer surface area.

Figure 3B shows the temperature counter for the cases with and without fins at different dimensions (the number and size of the fins are the same for all the cases) and at various times. The findings for the case without fins indicated that the PCM's temperature drops close to the wall, and the reduction temperature enlarges gradually. In contrast, the temperature of PCM remains higher than the HTF temperature. It is, therefore, unable to obtain thermal equilibrium even in the area close to the wall where it is solid. Since the fins operate as heat transfer bridges, transferring heat from the PCM to the HTF, and because they remain lower and higher than the PCM and the HTF, the fins never reach thermal equilibrium with the HTF at 5400 s for all the fins involved scenarios. Thermal conduction and buoyancy influence caused the PCM temperature to be greater at the top than at the bottom. It could be observed that the height of the fin has an impact factor in reducing the time needed for complete solidification.

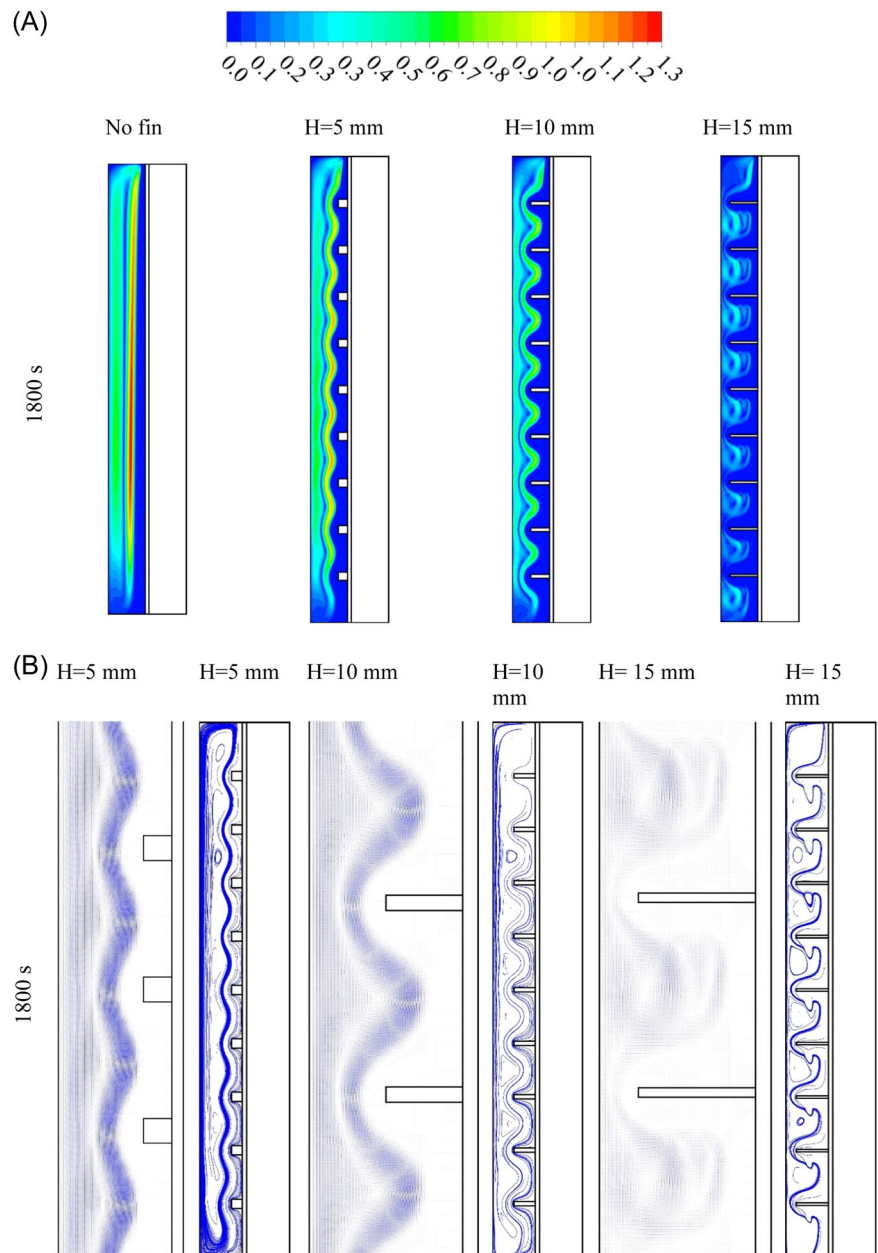
The velocity counter for four cases, including without fins and three different size fins ($H = 5, 10, 15$ mm) at the time of 1800 s, are presented in Figure 4A. For the case of no fins, the solidification PCM at the wall rises because of the difference in density between the liquid and the solid phases of the natural convection, which produces through the solidification process. The values of velocities at the solid region of PCM at the wall are about zero due to no flow moving at this region. However, far from this region, gradually, there are increases in the velocities and the maximum velocity seen between the solidification region of PCM and the liquid phase of PCM due to gradient temperature, which leads to heat transfer to create the solidification region. When adding fins, the solidification region of PCM increases more than without fin; hence the velocity near to wall is zero, and the region of gradient velocity increase with the decreased height of

fins. Also, the results refer to minimum gradient velocity observed with height fin = 15 mm compared to other cases with and without fins. Furthermore, the velocity vectors during the solidification processes of the systems with fins at different lengths ($H = 5$ mm, $H = 10$ mm, $H = 15$ mm) at the time of 1800 are displayed in Figure 4B. The results showed that the effect of the fins on velocity vectors and streamline around the fins where recirculation flow observed between every two fins due to solidification processes around the fins results in a difference in temperature between liquid and solid pages of PCM.

Figure 5A clarifies the development of the PCM's liquid fraction for different fins length cases and the finless case during the solicitation process. The trends of decrease in the liquid fraction of PCM are provided with the time of complete solidification (liquid fraction equals 0) could be observed and compared in this figure. The outcomes determine that the solidification process was completed faster (short time) with fins compared to the case without fins. Furthermore, the PCM's temperature profile for different fins length cases and the finless case during the solidification process are given in Figure 5B. It can be seen that it suddenly decreases at the initial stage of the solidification process due to the convection heat transfer generated in the liquid of PCM. The maximum temperature discloses that the solidification process happened initially, and the minimum temperature refers to developing complete solidification of PCM. The results detected that reducing the required time for completing the solidification process of PCM due to adding fins and the shorter time for the solidification process occurred at the length of fins $H = 15$ mm compared with other cases.

Table 3 presents the time of the PCM's solidification process for different fins length cases and the finless case. Note that the results of all proposed cases are presented in Table 2, which is discussed later. The results confirmed that the system's thermal performance rises as the system's height increases, and having fins (15 mm) shows the best argument concerning short time compared to all other cases. The primary heat transfer surface area for the most extended fins and heat delivery to the PCM's deepest section is responsible for this achievement. According to Table 3, the optimum case for the solidification time of 95% of the PCM is 97 min. This time is less than the cases with 5 and 10 mm fins and cases without fins by 80%, 65%, and 56%, respectively. The heat recovery rate for the case with the most extended fins is 27.66 W, which is greater than the cases without fins, with fins extending 5 and 10 mm, respectively, by 10.23, 13.25, and 18.48 W. The main objective from these results represented by using the most extended fins increases the system's average thermal conductivity while enhancing

FIGURE 4 (A) The velocity contours and (B) the stream factor of the liquid phase of the phase change material for various fin lengths at different time steps.



exchange surface area and the amount of heat delivered to the PCM domain.

5.2 | Effect of fin's number

Figure 6A demonstrates the impact of varying the number of fins (4, 9, 15, and 19 fins) on the solidification process while keeping the same volume of the fins in all cases. The solidification process begins along the wall and around the fins and increases due to discharging process of the PCM. The liquid PCM gradually diminishes over time as it divides into a liquid portion between every pair of fins for several fins (4 and 9) and a time of 5400 s.

However, this behavior is different at the number of fins (15 and 19) and time of 5400 s, where the liquid portion between every pair of fins becomes very small with fins (15) and disappears with fins (19). All cases demonstrate the same behavior pattern, which begins with a small layer of the solid PCM and then gradually increases along the wall and around the fins. The arrangement of the fins influences the PCM's discharging process at a uniform distance in two ways: first, the heat transmission to the PCM is more uniform; second, the lower and upper fins are located closer to the highest and lowest portions of the domain. Due to the effect of natural convection, the portion of unmelted PCM is higher at the top of the domain rather than that at the bottom. In addition,

increasing the surface area of the fins by using a higher number of fins promotes more significant heat removal from the PCM. Moreover, increasing the number of fins results in a more uniform heat sink distribution in the PCM domain.

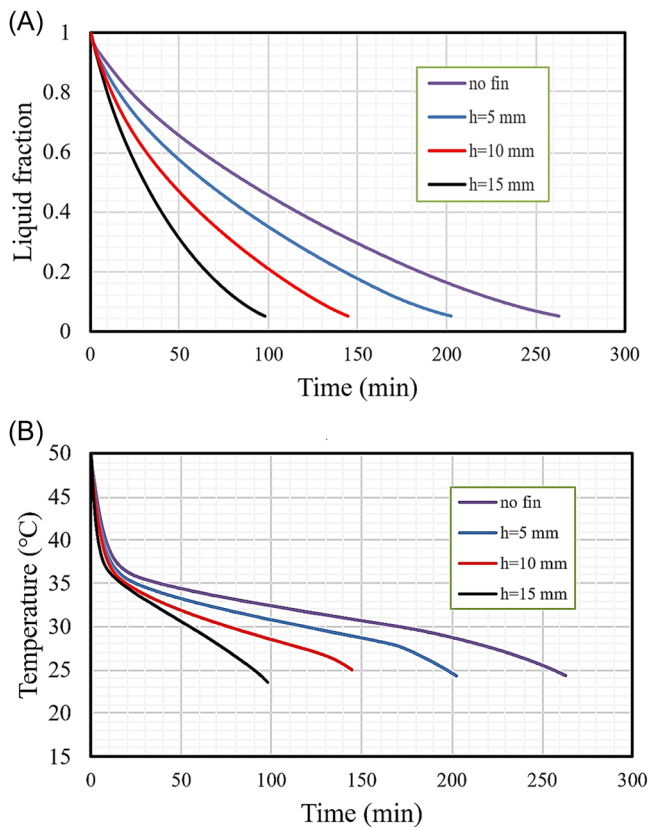


FIGURE 5 Decay of (A) the liquid fraction and (B) the mean temperature of the phase change material for different cases of the fins length during the melting process.

Figure 6B displays the temperature shape contours for the use of 4, 9, 15, and 19 fins for 5400 s. The PCM's temperature drops along the wall and around the fins in each case. In the case of the PCM with four fins and the early stage in the other cases, the fins do not reach thermal equilibrium with the PCM because they grow as the PCM discharges heat to HTF. In the most recent stages of the 15 and 19 fins scenarios, the temperature of the fins has nearly reached a steady state with the HTF. According to the findings, the PCM liquid is at its greatest temperature in the zone between each pair of fins at the beginning of the process.

As seen in Figure 7, adding more fins reduces movement and confines it to the spaces between neighboring fins. The barriers given by the fins, as they primarily control the movement of the liquid PCM, are the critical factor in this phenomenon. In the case of using four fins, there was little movement throughout the area at 1800 s of the solidification operation because of the large region between the two neighboring fins, and there was disappearing movement in the case of greater fins number because of the small areas between the fins. At 1800 s of the solidification operation, most of the PCM solids, and the slight movement observed all around the domain in the case of using four fins due to the wide area between the two neighbor fins and disappearing movement in the case of higher fins number due to limited areas between the fins.

Figure 8A shows the solidification process over time for various numbers of fins for 200 min. In each case, the solidification process was reduced significantly over time due to the heat transfer to the HTF being released. Through time, by the generation of a

Number of fins	Fin's height (mm)	Reynolds number	HTF temperature (°C)	Solidification time (s)	Heat recovery rate (W)
No fin		1000	15	15,784	10.23
9 fins	$H = 5$ mm	1000	15	12,152	13.29
9 fins	$H = 10$ mm	1000	15	8682	18.48
9 fins	$H = 15$ mm	1000	15	5884	27.66
4 fins	$H = 15$ mm	1000	15	10,025	17.07
15 fins	$H = 15$ mm	1000	15	4088	41.80
19 fins	$H = 15$ mm	1000	15	3541	48.1
19 fins	$H = 15$ mm	500	15	4065	42.03
19 fins	$H = 15$ mm	2000	15	3169	53.74
19 fins	$H = 15$ mm	1000	10	2877	57.73
19 fins	$H = 15$ mm	1000	20	4604	37.99

TABLE 3 The values of solidification time and heat recovery rate for different studied cases.

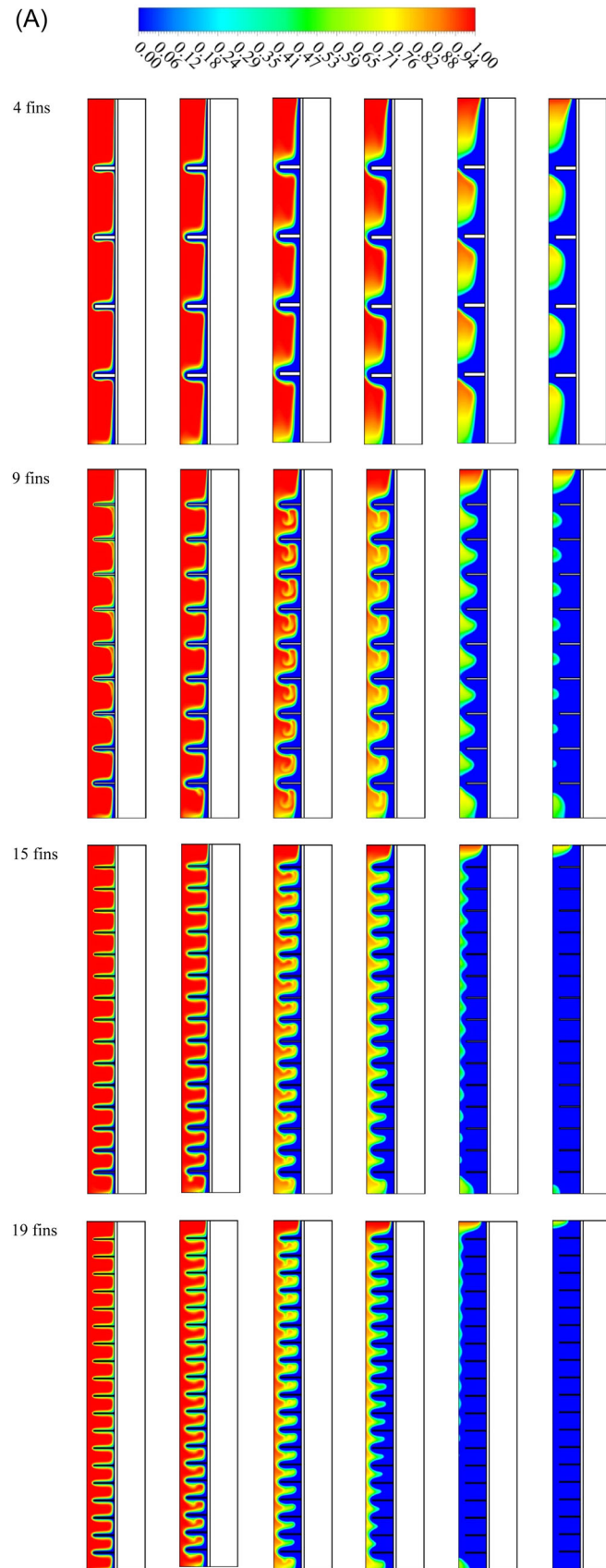


FIGURE 6 (A) Liquid fraction and (B) temperature distribution of the liquid phase of the phase change material for various fins numbers at different time steps.

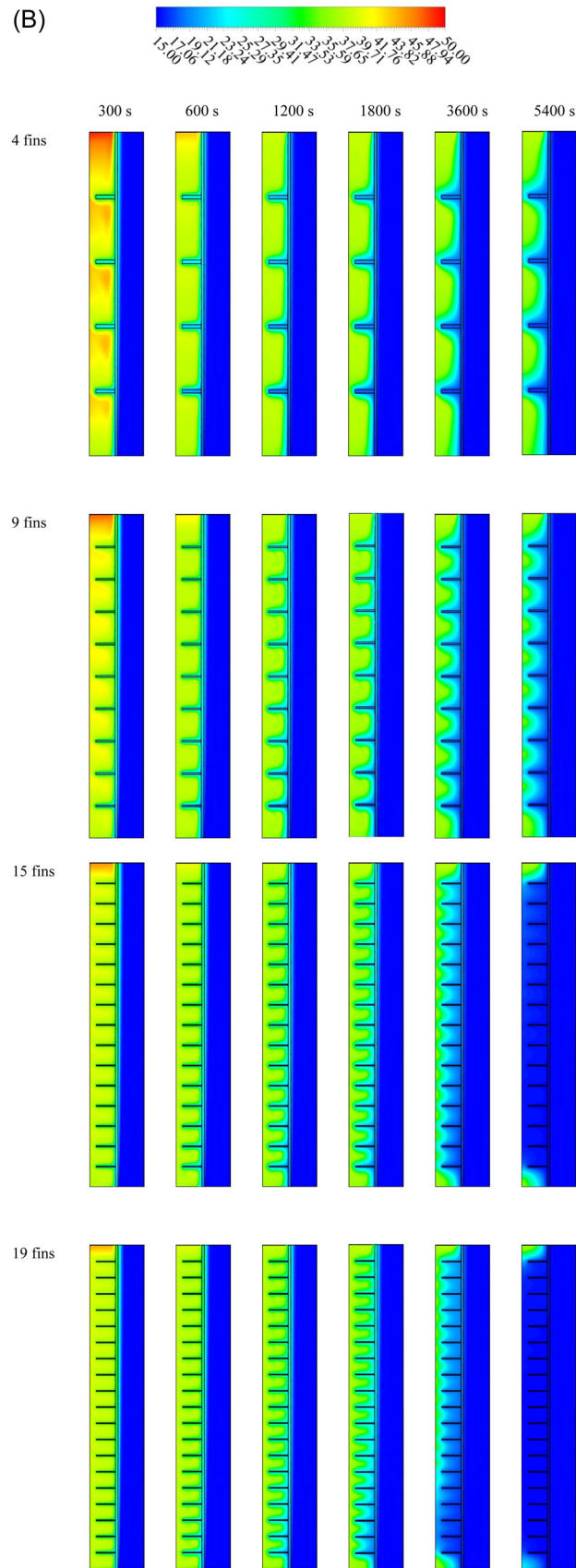


FIGURE 6 Continued

FIGURE 7 The velocity of the liquid phase of the phase change material for various fin numbers at the time of 1800 s.

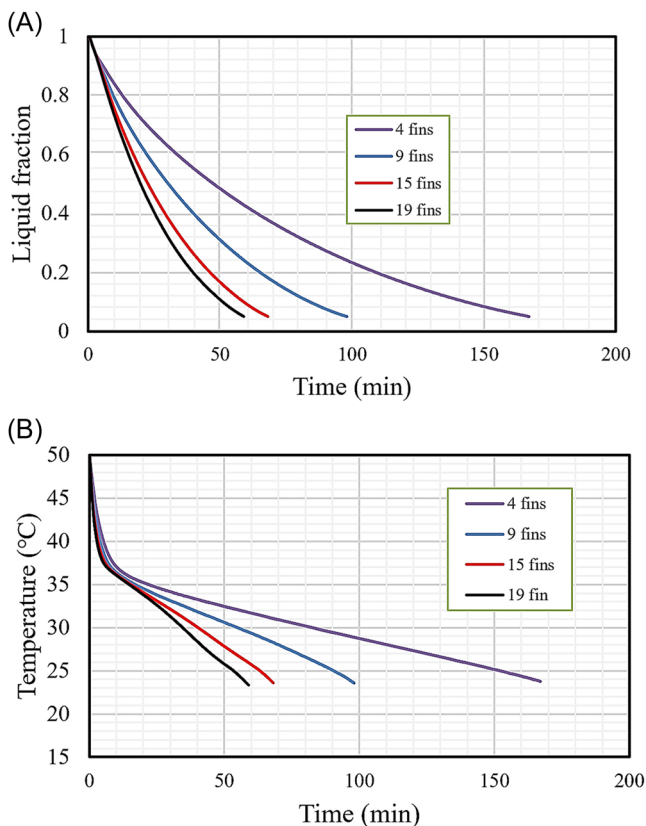
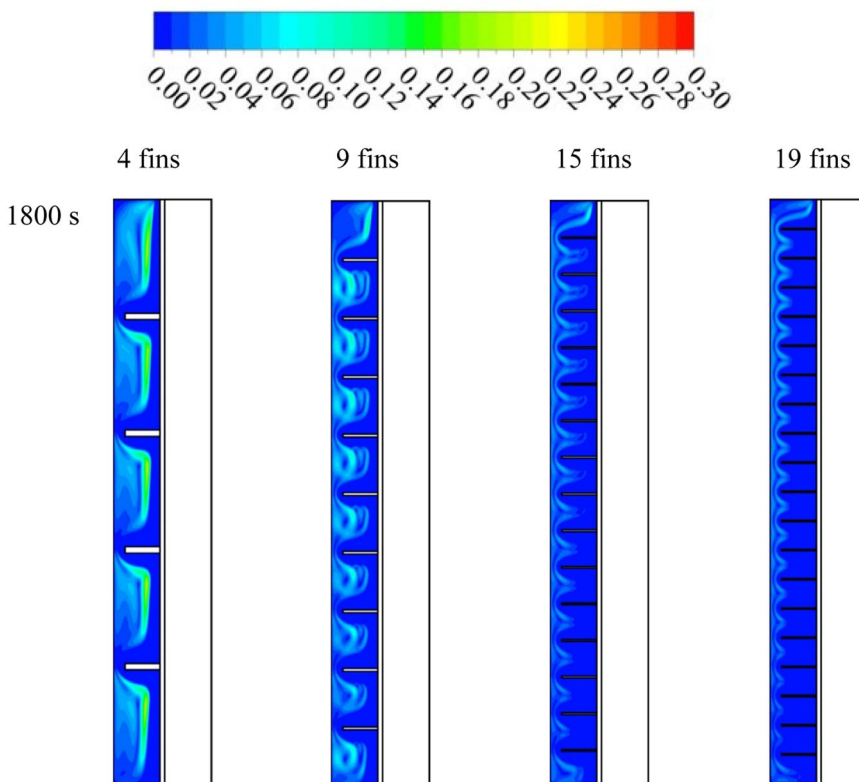


FIGURE 8 Decay of (A) the liquid fraction and (B) the mean temperature of the phase change material for different cases of the fins number during the melting process.

solid PCM layer near the walls, the rate of heat transfer (slope of the lines) reduces. The overall time for solidification in the case of utilizing four fins is 182 min. In contrast, in the case of employing 19 fins, the total solidification time is 88 min because the system with a higher number of fins has a more extensive heat transfer surface area.

Figure 8B shows that thermal conduction causes the mean temperature to drop significantly within the first period. The fins transfer heat from the PCM to the HTF, and the conduction effects heat the solid PCM near the walls. The mean temperature is lower than in the other cases at a given time because of the large surface area of the heat transfer in the case of using 19 fins. The average PCM temperatures are 24°C, 23.8°C, 23.6°C, and 23.2°C when the systems utilize 4, 9, 15, and 19 fins separately.

Due to the change in surface area and discharging process rate to the deep region of the PCM caused by the number of fins, the performance of solidification is affected by fin number. The casing with a high number of fins displays decreased solidification and an improvement in heat recovery rate due to the large surface area and improved thermal rate of the PCM. As shown in Table 3, the 19-fin case solidifies in 59 min less than the cases with 4, 9, and 15 fins. The heat recovery rates for 4, 9, 15, and 19 fins were 48.1, 41.8, 29.03, and 17.07 W, respectively.

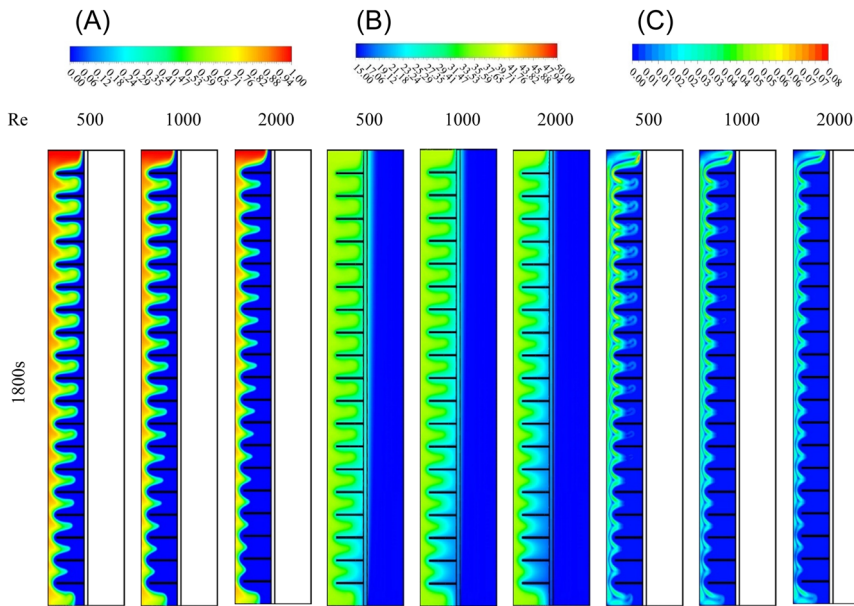


FIGURE 9 (A) The solidification process, (B) temperature, and (C) velocity distribution of the phase change material with various heat transfer fluids' Reynolds numbers at 1800 s.

5.3 | Effect of Reynold's number

The HTF flow rate, indicated by the Re number, impacts the PCM's solidification process. The PCM solidifies faster due to the greater flow rate and Re number providing the system with a constant cold fluid that constantly maintains the temperature differential between the PCM and the HTF as high as feasible. Moreover, the heat transfer coefficient enhances by increasing the Re number inside the HTF. The counter of the solidification process of the PCM for the case of the vastest and maximum number of fins with three values of Re (500, 1000, 2000) at the time of 1800 s illustrated in Figure 9A. The results indicated that in the case of a lower Re number, the region of liquid PCM remains confined between every two fins and at the top and bottom of the domain. In general, a rise in the Re number causes the PCM to solidify more quickly, compared to having less liquid PCM.

Figure 9B shows the counter temperature with different Reynolds flow rates of HTF for the case of 19 fins at the time of 1800 s. It is observed that a reduction in the temperature of PCM with an increase in the Reynolds number of HTF and the highest drop of temperature of PCM occurred with a Reynolds number of 2000 compared with other cases, which illustrates the solidification process of PCM.

Furthermore, Figure 9C shows the velocity counter of the PCM at 1800 s with various HTF Reynolds flow rates and for the case of 19 fins. The findings discovered that the increased Reynolds flow rate of HTF led to enlarge solid PCM region and a decrease in the liquid PCM zone, which represented the reduction in the laminar flow rate of the liquid phase of PCM for all cases.

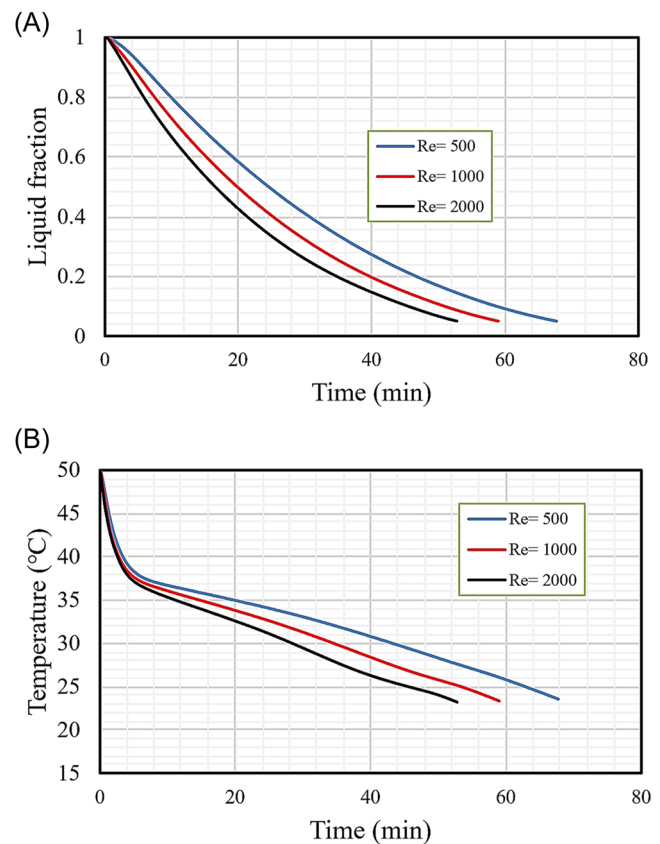
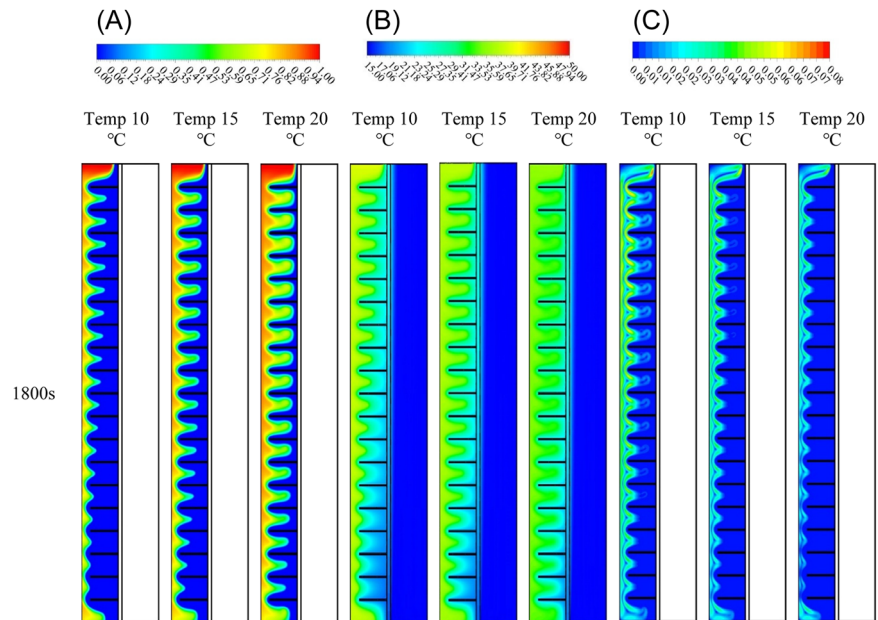


FIGURE 10 (A) The liquid fraction and (B) the mean temperature decay of the phase change material for different values of Re during the solidification process.

Figure 10A examines the influence of the HTF laminar flow rate as represented by different Reynolds numbers (Re)s (500, 1000, 2000) for the case of 19 fins. It has been discovered that increased flow rates

FIGURE 11 (A) The solidification process, (B) temperature, and (C) velocity distribution of the phase change material with various heat transfer fluids' inlet temperatures at 1800 s.



improve thermal efficiency and solidification. All curves have the same behavior where THE reduction liquid phase layer of PCM with increasing time. It is also observed that increasing Reynolds number of HTF flow rate affects the decreasing liquid phase layer of PCM and the required time for the solidification process. However, the required time for the solidification process with different Reynolds numbers represented 54 min for $Re = 2000$, 59 min for $Re = 1000$, and 68 min for $Re = 500$.

The mean temperature development of the PCM is presented in Figure 10B for the case of 19 fins and various Reynolds numbers (Re s) (500, 1000, 2000). The temperature differential between the HTF and the PCM is considerable with high Re , increasing the thermal exchange in the system, so the mean average temperature is directly proportional to the Re . Due to convective heat transfer, the temperature drops quickly during the initial stage of the discharging process before gradually decreasing, and the minimum temperature is detected.

The time of the solidification process and heat recovery rate of PCM at different Reynolds numbers (Re s) (500, 1000, 2000) were presented in Table 3. The results confirmed that the decreased time of the solidification process of PCM increases the Reynolds number. The optimum case for the solidification time was found at 53 min and a Reynolds number of 2000 compared with other cases. Moreover, the heat recovery rate for the case $Re = 2000$ is 53.74 W, which is greater than the rates for the cases $Re = 500$ and 100, respectively.

5.4 | Effect of different temperatures

The HTF temperature significantly impacts the phase change process in the TES units. Figure 11A represents the PCM's solidification process at 1800 s with different HTFs' inlet temperatures. The data demonstrates that the HTF with the lower temperature aids the PCM in solidifying more quickly due to the higher rate of heat transfer from PCM due to the increased temperature difference between the PCM and the HTF. In comparison, the increasing temperature of HTF leads to reduced solidification process of PCM due to decreases in the difference in temperature between the PCM and the HTF. Figure 11B, which also depicts the temperature distribution in the PCM for temperatures of 100°C, 150°C, and 200°C, reveals the same trend. The findings show that rising HTF temperature impacts PCM temperature distribution, with higher HTF temperatures leading to lower PCM temperatures and a delayed solidification process. Likewise, the effective temperature of HTF on the velocity counter has been presented in Figure 11C. The same behavior discussed above has been observed with different temperatures of HTF were seen at lower temperatures of HTF; there is recirculation flow between each fin due to convection heat transfer through the liquid phase of PCM and the difference in temperature between the PCM and the HTF.

Figure 12A shows the discharge processes using three different HTFs' inlet temperatures (10°C, 15°C, and 20°C). The graph demonstrates that the HTF inlet temperature directly affects the rate of the solidification process. HTF and PCM have a greater temperature

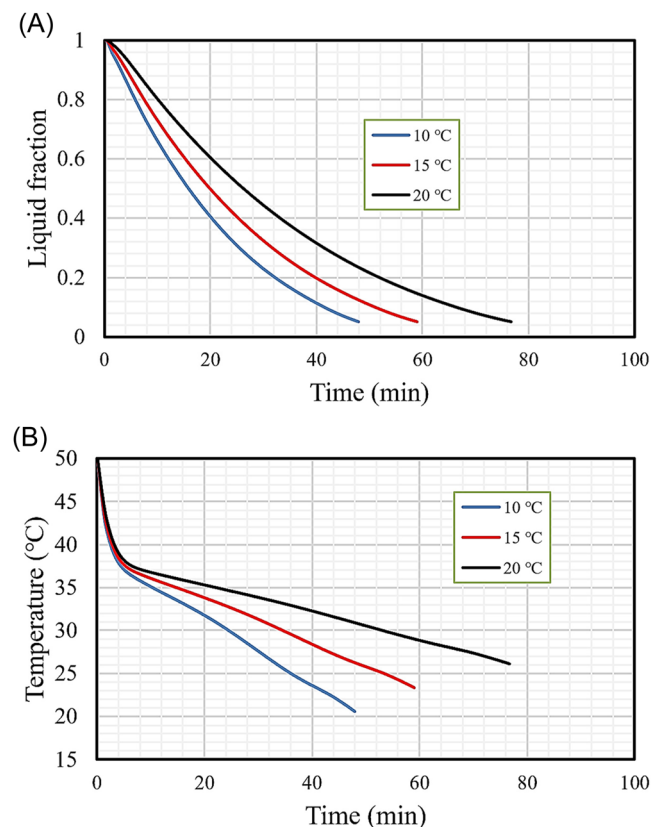


FIGURE 12 (A) Liquid fraction and (B) mean temperature decay of the phase change material for different values of heat transfer fluid inlet temperature during the solidification process.

difference since the HTF has a lower temperature. A faster rate of solidification results from the greater thermal exchange rate caused by the larger temperature differences. The solidification time increases by 48, 59, and 77 min, respectively, when the inlet temperature is raised from 10°C to 15°C and 20°C.

The PCMs' temperature decreases due to using the cooler HTF and reaching thermal equilibrium more quickly (Figure 12B). Since complete solidification rather than thermal equilibrium was considered when running the simulation, the conventional analysis was carried out until the PCM temperature reached 48°C.

To determine the required time of the solidification process with a different inlet temperature of HTF, the data was presented in Table 3. The minimum time for solidification PCM occurred at 49 min for inlet temperature 10°C, while in other cases with 15°C and 20°C the required time was 59 and 78 min, respectively. Heat recovery rates with different inlet temperatures of HTF were also presented in Table 2. This figure noted that the optimum heat recovery rate was 57.73 W at the inlet temperature of HTF of 10°C, but the other heat recovery rates were 48.15 and 37.99 at an inlet temperature of HTF of 15°C and 20°C.

6 | CONCLUSION

In this paper, TES system performance with and without fins have been compared numerically, as also the impacts of fin addition on the PCM solidification process. The main conclusions of the study are as follows:

- The efficiency of the solidification process is enhanced by adding fins to the TES system by increasing the area for heat transfer and the effective thermal conductivity, as the thermal conductivity of the metal fins is larger than that of the PCM.
- The addition of fins in the TES system impacted the streamlines and velocity vectors, causing recirculation flow during solidification, resulting in a temperature difference between the liquid and solid PCM sections. The velocities at the solid PCM region near the wall were close to 0 while increasing velocities were observed farther away from this region.
- The heat recovery rate for the case with the longest fins is 27.66 W, which is higher than the rates for cases without fins. While the cases with fins extending 5 and 10 mm, respectively, were 10.23, 13.25, and 18.48 W.
- The liquid PCM progressively decreases over time as it divides into a liquid portion between every pair of fins for fin numbers (4 and 9). Still, this behavior differs at fin numbers (15 and 19), where the liquid portion between every pair of fins becomes very small with fins (15) and disappears with fins (19).
- When the PCM is less liquid, and as the Re number increases, the PCM solidifies more quickly. Due to a higher heat transfer rate from the PCM and a larger temperature difference between the PCM and the HTF, the HTF with the lower temperature helps the PCM solidify more quickly. When the inlet temperature is increased from 10°C to 15°C and 20°C, the solidification times rise by 48, 59, and 77 min, respectively.

The impact of the materials used, the direction of the tubes and a wider variety of researched characteristics are all things the authors intend to look into in subsequent investigations. In addition, the researchers intend to manufacture the experimental design and conduct empirical work on the impacts of more complicated fins to improve heat transfer.

ORCID

Hayder I. Mohammed  <http://orcid.org/0000-0003-3647-3849>

Pouyan Talebizadehsardari  <http://orcid.org/0000-0001-5947-8701>

REFERENCES

- Ali HM. Phase change materials based thermal energy storage for solar energy systems. *J Build Eng.* 2022;56:104731.
- Zhao R, Dai H, Yao H. Liquid-metal magnetic soft robot with reprogrammable magnetization and stiffness. *IEEE Robot Autom Lett.* 2022;7:4535-4541.
- Huang G, Curt SR, Wang K, Markides CN. Challenges and opportunities for nanomaterials in spectral splitting for high-performance hybrid solar photovoltaic-thermal applications: a review. *Nano Mater Sci.* 2020;2:183-203.
- Chen K, Mohammed HI, Mahdi JM, Rahbari A, Cairns A, Talebizadehsardari P. Effects of non-uniform fin arrangement and size on the thermal response of a vertical latent heat triple-tube heat exchanger. *J Energy Storage.* 2022;45:103723.
- Ould Amrouche S, Rekioua D, Rekioua T, Bacha S. Overview of energy storage in renewable energy systems. *Int J Hydrogen Energy.* 2016;41:20914-20927.
- Yin X, Ye C, Ding Y, Song Y. Exploiting Internet data centers as energy prosumers in integrated Electricity-Heat system. *IEEE Trans Smart Grid.* 2023;14:167-182.
- He Y, Wang F, Du G, et al. Revisiting the thermal ageing on the metallised polypropylene film capacitor: from device to dielectric film. *High Voltage.* 2023;8(2):305-314.
- Niu J, Tian Z, Lu Y, Zhao H. Flexible dispatch of a building energy system using building thermal storage and battery energy storage. *Appl Energy.* 2019;243:274-287.
- Xia Y, Shi M, Zhang C, et al. Analysis of flexural failure mechanism of ultraviolet cured-in-place-pipe materials for buried pipelines rehabilitation based on curing temperature monitoring. *Eng Fail Anal.* 2022;142:106763.
- Chen L-Q, Zhao Y. From classical thermodynamics to phase-field method. *Prog Mater Sci.* 2022;124:100868.
- Ding M, Chen G, Xu W, et al. Bio-inspired synthesis of nanomaterials and smart structures for electrochemical energy storage and conversion. *Nano Mater Sci.* 2022;2:264-280.
- Lu X, Wang S. A GIS-based assessment of Tibet's potential for pumped hydropower energy storage. *Renew Sustain Energy Rev.* 2017;69:1045-1054.
- Lawag RA, Ali HM. Phase change materials for thermal management and energy storage: a review. *J Energy Storage.* 2022;55:105602.
- Tiji ME, Eisapour M, Yousefzadeh R, Azadian M, Talebizadehsardari P. A numerical study of a PCM-based passive solar chimney with a finned absorber. *J Build Eng.* 2020;32:101516.
- Pachori H, Choudhary T, Sheorey T. Significance of thermal energy storage material in solar air heaters. *Mater Today Proc.* 2022;56:126-134.
- Cabeza LF. Thermal energy storage. *Comprehensive Renewable Energy.* Vol 3. Elsevier; 2012:211-253.
- Rathod MK, Banerjee J. Thermal stability of phase change materials used in latent heat energy storage systems: a review. *Renew Sustain Energy Rev.* 2013;18:246-258.
- Yu J, Wang Y, Qi C, Zhang W. Solar thermal power generation characteristics based on metal foam and phase change materials doped with nanoparticles. *Colloids Surf A.* 2022;653:130001.
- Mohammed HI. Discharge improvement of a phase change material-air-based thermal energy storage unit for space heating applications using metal foams in the air sides. *Heat Transfer.* 2022;51:3830-3852.
- Khudhair AM, Farid M. A review on energy conservation in building applications with thermal storage by latent heat using phase change materials. In: Farid M, Auckaili A, Gholamibozanjani G, eds. *Thermal Energy Storage with Phase Change Materials.* 1st ed. CRC Press; 2021:162-175.
- Chatroudi IS, Atashafrooz M, Mohammed HI, Abed AM, Talebizadehsardari P. Heat transfer enhancement and free convection assessment in a double tube latent heat storage unit equipped with circular fins with optimum fin spacing. Evaluation of the melting process. *Front Energy Res;* 2023;11:3389.
- Bland A, Khzouz M, Statheros T, Gkanas E. PCMs for residential building applications: a short review focused on disadvantages and proposals for future development. *Buildings.* 2017;7:78.
- Sheikholeslami M, Haq R, Shafee A, Li Z, Elaraki YG, Tlili I. Heat transfer simulation of heat storage unit with nanoparticles and fins through a heat exchanger. *Int J Heat Mass Transfer.* 2019;135:470-478.
- Syednezhad M, Sheikholeslami M, Ali JA, Shafee A, Nguyen TK. Nanoparticles for water desalination in solar heat exchanger. *J Therm Anal Calorim.* 2020;139:1619-1636.
- Talebizadehsardari P, Mahdi JM, Mohammed HI, Moghimi MA, Hossein Eisapour A, Ghalambaz M. Consecutive charging and discharging of a PCM-based plate heat exchanger with zigzag configuration. *Appl Therm Eng.* 2021;193:116970.
- Ebrahimnataj Tiji M, Mohammed HI, Ibrahim RK, et al. Evaluation of T-shaped fins with a novel layout for improved melting in a triple-tube heat storage system. *Front Energy Res.* 2022;10:3389.
- Sun X, Mohammed HI, Tiji ME, et al. Investigation of heat transfer enhancement in a triple tube latent heat storage system using circular fins with inline and staggered arrangements. *Nanomaterials.* 2021;11:2647.
- Tiji ME, Al-Azzawi WK, Mohammed HI, et al. Thermal management of the melting process in a latent heat triplex tube storage system using different configurations of frustum tubes. *J Nanomater.* 2022;2022:7398110.
- Zhu Y, Xiao J, Chen T, et al. Experimental and numerical investigation on composite phase change material (PCM) based heat exchanger for breathing air cooling. *Appl Therm Eng.* 2019;155:631-636.
- Moore K, Wei W. Applications of carbon nanomaterials in perovskite solar cells for solar energy conversion. *Nano Mater Sci.* 2021;3:276-290.
- Qi C, Luo T, Liu M, Fan F, Yan Y. Experimental study on the flow and heat transfer characteristics of nanofluids in double-tube heat exchangers based on thermal efficiency assessment. *Energy Convers Manag.* 2019;197:111877.
- Khajuria S, Yadav A. Numerical investigation on the melting and solidification of Bio-PCM having annulus eccentricity in horizontal double pipe thermal energy storage. In: Patnaik A, Kukshal V, Agarwal P, Sharma A, Choudhary M, eds. *Application of Soft Computing Techniques in Mechanical Engineering.* CRC Press, 145-156.

33. Fallah Najafabadi M, Farhadi M, Talebi Rostami H. Numerically analysis of a phase-change material in concentric double-pipe helical coil with turbulent flow as thermal storage unit in solar water heaters. *J Energy Storage*. 2022;55:105712.
34. Ho CJ, Huang SH, Lai C-M. Enhancing laminar forced convection heat transfer by using Al_2O_3 /PCM nanofluids in a concentric double-tube duct. *Case Stud Therm Eng*. 2022;35:102147.
35. Selimefendigil F, Öztöp HF. Effects of using phase change material and non-Newtonian power law nanofluid on different sides of a double pipe heat exchanger for phase change dynamics and energy performance improvements. *Energy Storage*. 2022;4:e279.
36. Siavashi M, Miri Joibary SM. Numerical performance analysis of a counter-flow double-pipe heat exchanger with using nanofluid and both sides partly filled with porous media. *J Therm Anal Calorim*. 2019;135:1595-1610.
37. Pássaro J, Rebola A, Coelho L, et al. Effect of fins and nanoparticles in the discharge performance of PCM thermal storage system with a multi pass finned tube heat exchange. *Appl Therm Eng*. 2022;212:118569.
38. Abidi A, Rawa M, Khetib Y, Sindi HFA, Sharifpur M, Cheraghian G. Simulation of melting and solidification of graphene nanoparticles-PCM inside a dual tube heat exchanger with extended surface. *J Energy Storage*. 2021;44:103265.
39. Sanchouli M, Payan S, Payan A, Nada SA. Investigation of the enhancing thermal performance of phase change material in a double-tube heat exchanger using grid annular fins. *Case Stud Therm Eng*. 2022;34:101986.
40. Singh S, Kumar A, Singh P, Ansu A. Experimental analysis of double pipe heat exchanger with V-cut twisted tape inserts using PCM dispersed nanofluids. *Int J Veh Struct Syst*. 2022;14(2):179-184.
41. Ao C, Yan S, Hu W, Zhao L, Wu Y. Heat transfer analysis of a PCM in shell-and-tube thermal energy storage unit with different V-shaped fin structures. *Appl Therm Eng*. 2022;216:119079.
42. Deng S, Nie C, Jiang H, Ye W-B. Evaluation and optimization of thermal performance for a finned double tube latent heat thermal energy storage. *Int J Heat Mass Transfer*. 2019;130:532-544.
43. Baba MS, Raju AVSR, Rao MB. Heat transfer enhancement and pressure drop of Fe_3O_4 -water nanofluid in a double tube counter flow heat exchanger with internal longitudinal fins. *Case Stud Therm Eng*. 2018;12:600-607.
44. Salem MR, Eltoukhey MB, Ali RK, Elshazly KM. Experimental investigation on the hydrothermal performance of a double-pipe heat exchanger using helical tape insert. *Int J Therm Sci*. 2018;124:496-507.
45. Wijayanta AT, Yaningsih I, Aziz M, Miyazaki T, Koyama S. Double-sided delta-wing tape inserts to enhance convective heat transfer and fluid flow characteristics of a double-pipe heat exchanger. *Appl Therm Eng*. 2018;145:27-37.
46. Talebizadeh Sardari P, Walker GS, Gillott M, Grant D, Giddings D. Numerical modelling of phase change material melting process embedded in porous media: effect of heat storage size. *Proc Inst Mech Eng A J Power Energy*. 2020;234(3):365-383.
47. Mahdi JM, Nsofor EC. Melting enhancement in triplex-tube latent heat energy storage system using nanoparticles-metal foam combination. *Appl Energy*. 2017;191:22-34.
48. Shahsavar A, Khosravi J, Mohammed HI, Talebizadehsardari P. Performance evaluation of melting/solidification mechanism in a variable wave-length wavy channel double-tube latent heat storage system. *J Energy Storage*. 2020;27:101063.
49. Shahsavar A, Shaham A, Talebizadehsardari P. Wavy channels triple-tube LHS unit with sinusoidal variable wavelength in charging/discharging mechanism. *Int Commun Heat Mass Transfer*. 2019;107:93-105.
50. Wang P, Wang X, Huang Y, Li C, Peng Z, Ding Y. Thermal energy charging behaviour of a heat exchange device with a zigzag plate configuration containing multi-phase-change-materials (m-PCMs). *Appl Energy*. 2015;142:328-336.
51. Esapour M, Hosseini MJ, Ranjbar AA, Pahamli Y, Bahrampoury R. Phase change in multi-tube heat exchangers. *Renew Energy*. 2016;85:1017-1025.
52. Ye W-B, Zhu D-S, Wang N. Numerical simulation on phase-change thermal storage/release in a plate-fin unit. *Appl Therm Eng*. 2011;31:3871-3884.
53. Mahdi JM, Nsofor EC. Melting enhancement in triplex-tube latent thermal energy storage system using nanoparticles-fins combination. *Int J Heat Mass Transfer*. 2017;109:417-427.
54. Mat S, Al-Abidi AA, Sopian K, Sulaiman MY, Mohammad AT. Enhance heat transfer for PCM melting in triplex tube with internal-external fins. *Energy Convers Manag*. 2013;74:223-236.
55. Al-Abidi AA, Mat S, Sopian K, Sulaiman MY, Mohammad AT. Experimental study of melting and solidification of PCM in a triplex tube heat exchanger with fins. *Energy Build*. 2014;68:33-41.

How to cite this article: Bahlekeh A, Mouziraji HR, Togun H, et al. Evaluation of the solidification process in a double-tube latent heat storage unit equipped with circular fins with optimum fin spacing. *Energy Sci Eng*. 2023;11:2552-2570. doi:10.1002/ese3.1473